



## Molecular Crystals and Liquid Crystals

Publication details, including instructions for authors and subscription information:

<http://www.tandfonline.com/loi/gmcl20>

## Weak Anchoring Effects in Nematic Liquid Crystals

G. McKay<sup>a</sup>, K. J. Kidney<sup>a</sup> & I. W. Stewart<sup>a</sup>

<sup>a</sup> Department of Mathematics, University of Strathclyde, Glasgow, Scotland, United Kingdom

Version of record first published: 22 Sep 2010

To cite this article: G. McKay, K. J. Kidney & I. W. Stewart (2007): Weak Anchoring Effects in Nematic Liquid Crystals, *Molecular Crystals and Liquid Crystals*, 478:1, 57/[813]-66/[822]

To link to this article: <http://dx.doi.org/10.1080/15421400701683212>

PLEASE SCROLL DOWN FOR ARTICLE

Full terms and conditions of use: <http://www.tandfonline.com/page/terms-and-conditions>

This article may be used for research, teaching, and private study purposes. Any substantial or systematic reproduction, redistribution, reselling, loan, sub-licensing, systematic supply, or distribution in any form to anyone is expressly forbidden.

The publisher does not give any warranty express or implied or make any representation that the contents will be complete or accurate or up to date. The accuracy of any instructions, formulae, and drug doses should be independently verified with primary sources. The publisher shall not be liable for any loss, actions, claims, proceedings, demand, or costs or damages

whatsoever or howsoever caused arising directly or indirectly in connection with or arising out of the use of this material.

## Weak Anchoring Effects in Nematic Liquid Crystals

G. McKay  
K. J. Kidney  
I. W. Stewart

Department of Mathematics, University of Strathclyde, Glasgow,  
Scotland, United Kingdom

*We consider a twisted nematic liquid crystal confined by two parallel boundary plates. The nematic is subject to an in-plane magnetic field applied in a direction parallel to the plates. At the lower plate the director is strongly anchored so that the director twist is fixed. On the upper surface we introduce an easy direction for the director. Although the director prefers to align with the easy direction, the actual twist exhibited at the upper surface may differ from the easy direction twist. This is due to the competition between elastic, magnetic and anchoring effects. We examine and compare two surface energies that model the weak anchoring at the upper plate. For both energies, equilibrium twist profiles for the director within the sample have been obtained by minimizing the total free energy for the system.*

**Keywords:** continuum modelling; nematic liquid crystals; weak anchoring

## INTRODUCTION

We consider an incompressible nematic liquid crystal, infinite in the  $xy$ -plane and constrained in the  $z$ -direction by two parallel glass plates a distance  $d$  apart. The average molecular alignment in the nematic is described by the usual director  $\mathbf{n}$ , a unit vector. It will be assumed that the director alignment on both boundary plates will always remain parallel to the plates. Under the influence of an externally applied magnetic field, the director may exhibit a twist angle  $\phi(z)$  across the depth of the cell, as shown in Figure 1. It is therefore natural to

Address correspondence to G. McKay, Department of Mathematics, University of Strathclyde, 26 Richmond St., Glasgow, G1 1XH, Scotland, U.K. E-mail: gmck@maths.strath.ac.uk

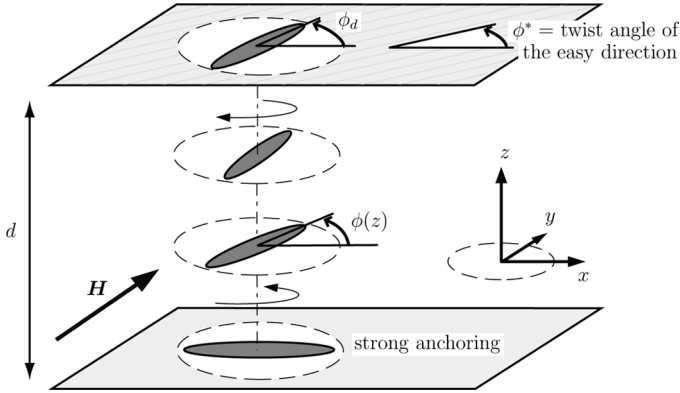


**FIGURE 1** Schematic showing the twisted nematic liquid crystal with its director always parallel to the plates. The liquid crystal is subject to an in-plane magnetic field in the  $y$ -direction.

suppose that, by the geometry described in Figure 1,

$$\mathbf{n} = (\cos \phi(z), \sin \phi(z), 0), \quad 0 \leq z \leq d. \quad (1)$$

A magnetic field  $\mathbf{H} = H(0, 1, 0)$  of magnitude  $H$  is applied in the  $y$ -direction parallel to the plates. At the lower plate the director is strongly anchored so that the director is given by  $\mathbf{n}_0 = (1, 0, 0)$  at  $z = 0$ , which corresponds to the boundary condition

$$\phi(0) = 0. \quad (2)$$

By carefully rubbing the upper plate in one direction only, the director can be encouraged to align along the rubbing direction induced on the plate. This direction of rubbing is sometimes referred to as the *easy axis* and the director is said to be aligned along an *easy direction*. Here we introduce an easy direction along the upper surface which corresponds to the twist angle  $\phi^*$ ,  $0^\circ \leq \phi^* \leq 90^\circ$ , as indicated in Figure 1. Although the director prefers to align with a twist equal to this easy direction, the actual twist exhibited at the upper surface,  $\phi_d$ , may differ from  $\phi^*$ : this is due to the competition between elastic and magnetic effects in the bulk of the sample, the strong anchoring at the lower plate and the preferred upper surface orientation.

Equilibrium profiles for the director within the sample can be obtained by minimizing the total free energy for the system. It is straightforward to show that the bulk nematic elastic energy density contribution,  $w_{\text{elas}}$ , associated with the above twist configuration can

be written as [1]

$$w_{\text{elas}} = \frac{1}{2} K_2 (\mathbf{n} \cdot \nabla \times \mathbf{n})^2 = \frac{1}{2} K_2 (\phi')^2, \quad (3)$$

where  $K_2 > 0$  is the twist elastic constant and  $'$  denotes  $d/dz$ . The bulk magnetic energy density is given by [1]

$$w_{\text{mag}} = -\frac{1}{2} \chi_a (\mathbf{n} \cdot \mathbf{H})^2 = -\frac{1}{2} \chi_a \sin^2 \phi, \quad (4)$$

where  $\chi_a$  is the magnetic anisotropy. We shall assume that  $\chi_a > 0$ , which indicates that the director prefers to align parallel to the applied field direction. The total bulk energy density  $w_b$  that is relevant here is simply

$$w_b = w_{\text{elas}} + w_{\text{mag}}. \quad (5)$$

The total energy for the system consists of the sum of the bulk and surface energies.

The aim of this article is to examine two different representations of the weak azimuthal anchoring energy density at the upper plate. The simplest surface energy density, first proposed by Rapini and Papoular [1,2], can be expressed in our notation as

$$w_{\text{RP}} = \frac{1}{2} \tau_0 (1 + \omega \sin^2(\phi - \phi^*)), \quad (6)$$

where  $\tau_0 > 0$ ,  $\omega > 0$  is a dimensionless anchoring parameter and  $\phi^*$ , as introduced earlier, is the angle corresponding to the easy direction on the upper boundary. The anchoring strength is  $\tau_0 \omega$  ( $\text{Nm}^{-1}$ ). Clearly, this surface energy density can achieve its absolute minimum if  $\phi = \phi^*$ , i.e. if the director at the surface coincides with the easy direction. Recently, however, Belyakov *et al.* [3–5] proposed an alternative form for a weak anchoring energy density that is particularly relevant to twist geometries. In our notation, this alternative version may be written as

$$w_{\text{RP}} = \frac{1}{2} \tau_0 \left( 1 + 4\omega \sin^2 \left( \frac{\phi - \phi^*}{2} \right) \right). \quad (7)$$

We shall refer to (6) and (7) as the RP and B surface energy densities, respectively. The physical motivation for the B form of surface energy is largely driven by pitch ‘jumps’ in cholesteric liquid crystals where the twist of the director is dominant and is related to the twist elastic constant  $K_2$  [3–5]. By considering simple series expansions, it can be shown that the RP and B energies almost coincide when the actual

surface twist angle is close to the easy direction  $\phi^*$ . However, we expect the bulk equilibrium twist profiles exhibited by our system to be dependent upon the choice of weak anchoring energy, as will be discussed below.

In the following analysis we use  $w_s$  to denote either  $w_{\text{RP}}$  or  $w_{\text{B}}$ . Combining Eqs. (3)–(7) above, we can now calculate  $W$ , the total free energy for our system, as

$$W = \int_V w_b dV + \int_S w_s dS. \quad (8)$$

Here  $V$  represents the volume of our sample and  $S$  is the upper surface  $z = d$ . (Strong anchoring on the lower surface will not introduce any additional finite surface energy.) Equilibrium twist profiles correspond to minimizers of (8). The corresponding Euler-Lagrange equation in the bulk of the sample is

$$\frac{d}{dz} \left( \frac{\partial w_b}{\partial \phi'} \right) - \frac{\partial w_b}{\partial \phi} = 0. \quad (9)$$

Furthermore, we can derive a boundary condition for the twist at the surface  $z = d$  by invoking the balance of couple condition [6] (also cf. p. 56 in Stewart [1])

$$\frac{\partial w_b}{\partial \phi'} + \frac{\partial w_s}{\partial \phi} = 0 \quad \text{at } z = d. \quad (10)$$

The solution of (9) subject to the boundary conditions (2) and (10) delivers the complete solution for  $\phi(z)$  to our problem.

By rescaling coordinate  $z \rightarrow z/d$  and employing Eqs. (3)–(7), we can rewrite the equilibrium equation (9) and boundary conditions (2), (10) in terms of the twist angle  $\phi$  for the dimensionless variable  $z$  with  $0 \leq z \leq 1$ . Doing so gives

$$\phi'' + \pi^2 \frac{H^2}{H_c^2} \cos \phi \sin \phi = 0 \quad \text{for } 0 < z < 1; \quad (11)$$

$$\phi = 0 \quad \text{at } z = 0; \quad (12)$$

$$\left. \begin{array}{l} \text{RP: } \phi' + \frac{\pi}{2\rho} \sin(2(\phi - \phi^*)) = 0 \\ \text{B: } \phi' + \frac{\pi}{\rho} \sin(\phi - \phi^*) = 0 \end{array} \right\} \quad \text{at } z = 1. \quad (13)$$

The two boundary conditions stated in (13) correspond to either of the RP or B surface energies. Two parameters have been introduced in

(11) and (13), namely

$$H_c = \frac{\pi}{d} \sqrt{\frac{K_2}{\chi_a}} \quad \text{and} \quad \rho = \frac{K_2 \pi}{d \tau_0 \omega}. \quad (14)$$

The quantity  $H_c$  denotes the critical magnetic field strength for a Freedericksz transition in a cell with strong anchoring on both plates, while the parameter  $\rho$  is a measure of the relative strength of the elastic and surface energy contributions (see Stewart [1], p. 78 and p. 98, respectively). For example, large values of  $\rho$  correspond to very weak anchoring at the upper surface.

## EQUILIBRIUM PROFILES

### (i) $H = 0$

To help demonstrate some of the differences between the RP and B surface energies, we first consider the system of equations (11)–(13) in the absence of a magnetic field, i.e. when  $H = 0$ . Recall that earlier we introduced  $\phi_d$  as the actual twist angle exhibited by the director at the upper surface. It is straightforward to show that when  $H = 0$  the equilibrium solution must take the form  $\phi(z) = \phi_d z$  ( $0 \leq z \leq 1$ ). In order to calculate the surface twist  $\phi_d$  we substitute this linear profile for  $\phi(z)$  into either one of the boundary conditions (13). Therefore,  $\phi_d$  can be found for either the RP or B surface energies by solving the appropriate equations

$$\text{RP: } \phi_d + \frac{\pi}{2\rho} \sin(2(\phi_d - \phi^*)) = 0, \quad (15)$$

$$\text{B: } \phi_d + \frac{\pi}{\rho} \sin(\phi_d - \phi^*) = 0. \quad (16)$$

First consider the particular situation when the easy axis is  $\phi^* = 90^\circ$ . The solutions to the boundary requirements (15) and (16) when  $\phi^* = 90^\circ$  are depicted in Figure 2. In this case, from (15) the RP energy allows an upper surface twist  $\phi_d = 0^\circ$  that is independent of the choice of anchoring strength parameter  $\rho$ . Furthermore, below a critical value of the anchoring parameter  $\rho$  it is also possible to find non-zero solutions to (15) with the upper surface twist much closer to the easy direction  $\phi^*$ . By considering (15) in the limit as  $\phi_d \rightarrow 0$  we can show that this critical value of the anchoring parameter is  $\rho = \pi$ . In contrast, the surface condition (16) for the B energy never allows trivial solutions (except in the limiting case as  $\rho \rightarrow \infty$ ).

Now consider the case when  $\phi^* < 90^\circ$ . In particular, in Figure 3 we consider the cases  $\phi^* = 89^\circ$  and  $\phi^* = 45^\circ$ . The trivial solution  $\phi_d = 0^\circ$  is

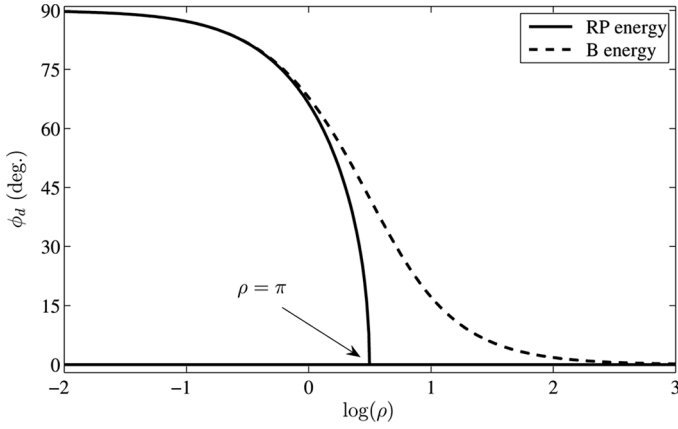


**FIGURE 2** The dependence of the upper surface twist  $\phi_d$  upon the anchoring parameter  $\rho$  when  $\phi^* = 90^\circ$  and  $\mathbf{H} = \mathbf{0}$ . The solid lines represent the two possible solutions for the RP energy and the dashed line represents that for the B energy.

no longer possible for the RP equation in (15). It can be seen that as the anchoring strength  $\tau_0\omega$  increases (i.e. as  $\rho$  decreases), the values of  $\phi_d$  approach the easy direction  $\phi^*$  and that, conversely, for very weak anchoring (large  $\rho$ ), the angle  $\phi_d$  is close to  $0^\circ$ . Furthermore, from Figure 3 we see that as  $\phi^*$  decreases the difference between

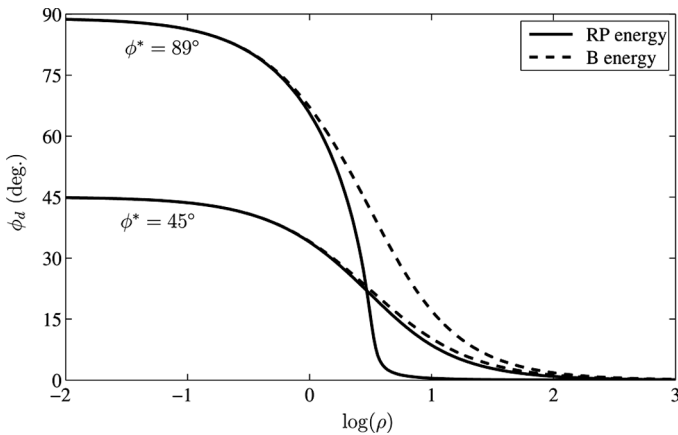


**FIGURE 3** The dependence of the upper surface twist  $\phi_d$  upon the anchoring parameter  $\rho$  when  $\mathbf{H} = \mathbf{0}$  and  $\phi^* = 45^\circ$  or  $89^\circ$ .



the graphs of  $\phi_d$  for the RP and B energy densities decreases, i.e. as  $\phi^* \rightarrow 0$  the two energies lead to similar values for  $\phi_d$ .

## (ii) $H \neq 0$

Now we return to the case when the magnetic field is present, i.e.  $H \neq 0$ . Analytical solutions to the system of Eqs. (11)–(13) for both types of weak anchoring will now be sought. Millar and McKay [7] examined the director orientation of a twisted nematic liquid crystal subject to a net twist across the layer. Although the model considered by these authors is very different to that considered here, we can apply a similar analysis and approach. Specifically, two types of solution are possible for either weak anchoring condition. The first has a monotonic profile where  $\phi'$  is positive throughout the bulk of the sample, irrespective of the magnitude of the magnetic field. By considering either version of boundary condition (13), we can conclude that for these monotonic profiles  $0 \leq \phi_d \leq \phi^*$  (since  $\phi(1) > 0$ ). When the surface anchoring strength term  $\tau_0\omega$  is large (i.e.,  $\rho$  is small) the angle  $\phi_d$  will be slightly smaller than the easy direction  $\phi^*$ , but cannot necessarily be equal to  $\phi^*$  due to the additional influences from bulk elastic and field effects. Therefore this first type of solution corresponds to the case where  $\phi_d$  is actually the maximum twist calculated for the director across the sample.

A second type of non-monotonic solution can occur when the field strength is sufficiently large. This behaviour is the result of the competition between the magnetic field and surface anchorings. These non-monotonic solutions are characterized by a maximum which occurs at some point  $z \in (0, 1)$ . The transition from a monotonic increasing solution to non-monotonic solution occurs at a critical field strength,  $\hat{H}$ , where the solution  $\phi(z)$  satisfies

$$\phi'(1) = 0 \quad \text{and} \quad \phi_d \equiv \phi(1) = \phi^*. \quad (17)$$

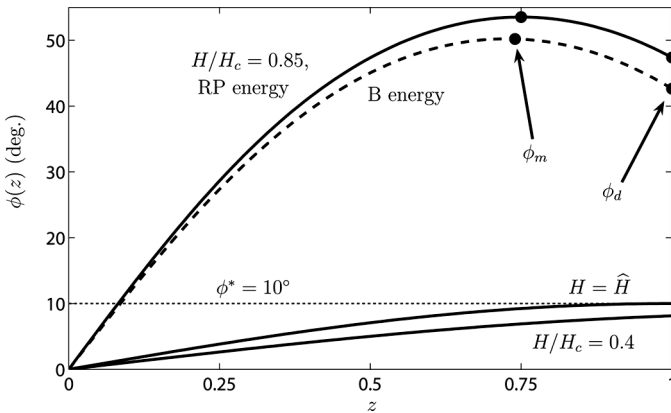
We can obtain an analytical expression for  $\hat{H}$  by solving Eq. (11) subject to the boundary conditions (12) and (17). We note that this critical field strength is independent of the form adopted for the weak anchoring energy. Following an analysis similar to Stewart [1] or Millar and McKay [7], our approach involves multiplying (11) by  $\phi'$ , integrating to obtain the corresponding first integral, and then applying the appropriate boundary conditions. Consequently, we find that the critical transition field strength  $\hat{H}$  can be calculated in terms of the easy direction  $\phi^*$  via

$$\frac{\hat{H}}{H_c} = \frac{1}{\pi} \int_0^{\phi^*} \frac{d\hat{\phi}}{(\sin^2 \phi^* - \sin^2 \hat{\phi})^{1/2}} = \frac{1}{\pi} K(\sin \phi^*), \quad (18)$$

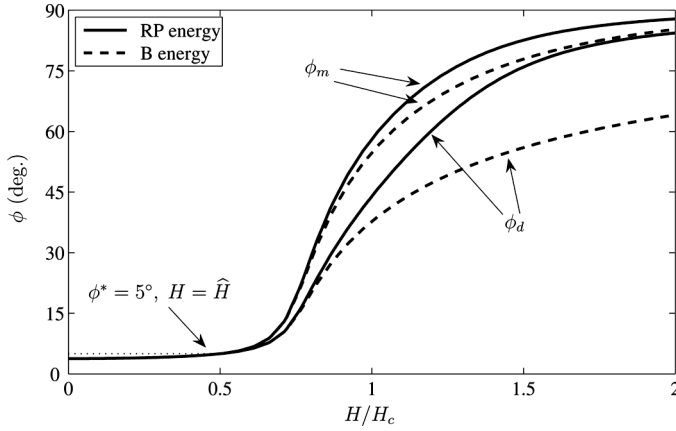
where  $H_c$  is defined in Eq. (14) and  $K(\cdot)$  is the complete elliptic integral of the first kind. The second equality in (18) is obtained by the usual Zocher [1] substitution  $\sin \hat{\phi} = \sin \phi^* \sin \lambda$  ( $0 \leq \lambda \leq \pi/2$ ) in the integral that appears in (18).

Figure 4 illustrates different twist solution profiles for  $\phi(z)$  for the system of equations (11)–(13) as the field strength  $H$  is varied. For the particular value of  $\phi^* = 10^\circ$  we have plotted the twist solution  $\phi(z)$  when  $H = \hat{H}$ , where  $\hat{H}$  is calculated via the relation (18) (in this particular case  $\hat{H}/H_c \approx 0.504$ ), and for values of  $H$  that are above and below  $\hat{H}$ . It is clear that the monotonically increasing solutions are available for  $H < \hat{H}$  while the non-monotonic solutions appear for  $H > \hat{H}$ . For  $H \leq \hat{H}$  the solutions for the RP and B formulations are very similar. (In fact, in Fig. 4 the RP and B solutions are indistinguishable for  $H \leq \hat{H}$ .) Nevertheless, there is a marked difference between the solutions for the RP and B cases when  $H$  is above  $\hat{H}$ . Although it is possible to derive these profiles analytically using the methods detailed in Stewart [1], here we have calculated  $\phi(z)$  numerically by solving the boundary value problem given by Eqs. (11)–(13).

In Figure 5 we consider  $\phi^* = 5^\circ$ ,  $\rho = 1$  and characterize the twist profile solutions of (11)–(13) for the RP and B energies via two angles. The first is simply the upper surface twist previously defined as  $\phi_d$ . The second angle,  $\phi_m$ , is the maximum twist angle exhibited by the solution across the whole cell. Following our earlier discussion, the angles  $\phi_d$  and  $\phi_m$  will coincide for  $H \leq \hat{H}$ . As the magnetic field



**FIGURE 4** Solution profiles for magnetic field strengths  $H/H_c = 0.4$ ,  $H = \hat{H}$  and  $H/H_c = 0.85$  when  $\phi^* = 10^\circ$  and  $\rho = 1.75$ . Note, for the cases  $H/H_c = 0.4$  and  $H = \hat{H}$  the RP and B energy solutions are indistinguishable.



**FIGURE 5** Surface twist angles,  $\phi_d$ , and maximum twist angles,  $\phi_m$ , as the magnetic field strength  $H$  varies,  $\phi^* = 5^\circ$  and  $\rho = 1$ .

strength increases the two angles  $\phi_d$  and  $\phi_m$  increase towards the limiting value  $\phi = 90^\circ$  that minimizes the bulk magnetic energy density  $w_{\text{mag}}$ . However, the angles corresponding to the RP and B energies also diverge as  $H/H_c$  increases. In particular, for a fixed magnetic field  $H \gg H_c$  and fixed surface anchoring strengths, twist profiles for the B energy exhibit angles smaller than the equivalent RP solutions, as shown in Figure 5. The discrepancy between the two energies is most significant at the upper surface when the field strength is high.

## DISCUSSION

As mentioned previously, the two surface energies we consider here are very similar in behaviour provided the director on the upper plate is close to the easy direction. However, as the magnetic field strength increases, the director in the bulk prefers to align with the field. Consequently, the twist at the upper surface is forced away from its optimal easy direction. Figures 4 and 5 are very significant because they emphasize the differences between the RP and B energies at these large field strengths. The B potential appears to be more effective at maintaining a surface twist  $\phi_d$  close to the easy direction  $\phi^*$ . The analysis and calculations presented here can be compared directly with experimental measurements for  $\phi_d$  in order to validate the correct choice of azimuthal surface energy when modelling twisted nematic liquid crystals.

Both the RP and B energies ought to be modified by the addition of fourth or higher order contributions when deviations of the director away from the easy axis become large. Such an approach has been investigated by Yokoyama and van Sprang [8] in the context of an RP-type energy and a similar methodology may be appropriate for the B energy. More realistic comparisons between the RP and B-type energies for large deviations of the director will then be possible.

## REFERENCES

- [1] Stewart, I.W. (2004). *The Static and Dynamic Continuum Theory of Liquid Crystals*, Taylor and Francis: London and New York.
- [2] Rapini, A. & Papoular, M. (1969). *J. de Physique Colloq.*, 30(C4), 54–56.
- [3] Belyakov, V. A., Stewart, I. W., & Osipov, M. A. (2004). *JETP*, 99, 73–82.
- [4] Belyakov, V. A., Stewart, I. W., & Osipov, M. A. (2005). *Phys. Rev. E*, 71, 051708.
- [5] Belyakov, V. A., Osipov, M. A., & Stewart, I. W. (2006). *J. Phys.: Condens. Matter*, 18, 4443–4460.
- [6] Jenkins, J. T. & Barratt, P. J. (1974). *Q. Jl. Mech. Appl. Math.*, 27, 111–127.
- [7] Millar, H. & McKay, G. (2005). *Mol. Cryst. Liq. Cryst.*, 435, 937–946.
- [8] Yokoyama, H. & van Sprang, H. A. (1985). *J. Appl. Phys.*, 57, 4520–4526.